Gain Without Pain: Accurate WiFi-based Localization using Fingerprint Spatial Gradient

CHENSHU WU, School of Software, Tsinghua University
JINGAO XU, School of Software, Tsinghua University
ZHENG YANG, School of Software, Tsinghua University
NICHOLAS D. LANE, University College London and Bell Labs
ZUWEI YIN, School of Software, Tsinghua University

Among numerous indoor localization systems proposed during the past decades, WiFi fingerprint-based localization has been one of the most attractive solutions, which is known to be free of extra infrastructure and specialized hardware. However, current WiFi fingerprinting suffers from a pivotal problem of RSS fluctuations caused by unpredictable environmental dynamics.The RSS variations lead to severe spatial ambiguity and temporal instability in RSS fingerprinting, both impairing the location accuracy. To overcome such drawbacks, we propose *fingerprint spatial gradient* (FSG), a more stable and distinctive form than RSS fingerprints, which exploits the spatial relationships among the RSS fingerprints of multiple neighbouring locations.As a spatially relative form, FSG is more resistant to RSS uncertainties. Based on the concept of FSG, we design novel algorithms to construct FSG on top of a general RSS fingerprint database and then propose effective FSG matching methods for location estimation. Unlike previous works, the resulting system, named ViVi, yields performance gain without the pains of introducing extra information or additional service restrictions or assuming impractical RSS models. Extensive experiments in different buildings demonstrate that ViVi achieves great performance, outperforming the best among four comparative start-of-the-art approaches by 29% in mean accuracy and 19% in 95th percentile accuracy and outweighing the worst one by 39% and 24% respectively. We envision FSG as a promising supplement and alternative to existing RSS fingerprinting for future WiFi localization.

CCS Concepts: •**Human-centered computing →Ubiquitous and mobile computing;**

Additional Key Words and Phrases: Indoor Localization; WiFi Fingerprint; Spatial Gradient

ACM Reference format:
Chenshu Wu, Jingao Xu, Zheng Yang, Nicholas D. Lane, and Zuwei Yin. 2017. Gain Without Pain: Accurate WiFi-based Localization using Fingerprint Spatial Gradient . *PACM Interact. Mob. Wearable Ubiquitous Technol.* 0, 0, Article 0 (February 2017), 19 pages.
DOI: http://doi.org/10.1145/3090094

1 INTRODUCTION

The proliferation of various location-based ubiquitous applications fosters the demand for accurate localization services to be available everywhere. Numerous techniques have been developed during the past decades based

This work is supported by the NSF China Grant No. 61672319 and No. 61632008.
Authorfis address: C. Wu, J. Xu, Z. Yang, Z. Yin, Room 11-211, East Main Building, Tsinghua University, Beijing, China 100084; email: {wucs32, xujingao13, hmilyyz, yinzw81}@gmail.com. N. D. Lane, email: niclane@acm.org.

DOI: http://doi.org/10.1145/3090094

on WiFi [47], RFID [36], acoustic signals [23], visual images [42], and inertial sensors [14], etc. Among various approaches, WiFi fingerprint-based indoor localization has become one of the most attractive solutions due to the wide deployment and availability of WiFi infrastructure [13, 20, 22, 28, 30, 34, 43, 47]. Great companies including Apple, Cisco, Huawei, and Baidu etc have all built or invested and are still developing related products. Such schemes leverage Received Signal Strengths (RSSs) of WiFi signals as location fingerprints and typically employ smartphones as clients, rendering them free of extra infrastructure and specialized devices and feasible for large-scale deployment.

Typically, fingerprint-based approaches consist of two stages. In the first training phase, fingerprints are collected with known location labels to form a fingerprint database (a.k.a radio map). Then during the localization stage, user location is determined by matching fingerprint observation against those stored in the fingerprint database. The training phase is usually completed by site survey, which is labour-intensive and time-consuming [44] and was considered a major hurdle for real applications. Recent advances in mobile crowdsourcing have eased this task by automatically constructing the fingerprint database, making fingerprint-based approaches even attractive for practical deployment [28, 34, 43, 44]. However, existing RSS fingerprint-based systems still suffer from several drawbacks, especially in the perspective of localization accuracy.

Many applications demand for precise locations for refined advertisements, staff managements, exhibits monitoring, etc. Existing techniques, however, frequently yield large errors of up to ten meters in practice [24]. One major root cause of the locations errors in RSS fingerprinting is the RSS uncertainty of WiFi signals. RSS is known to be vulnerable to unpredictable environmental dynamics, especially in complex indoor environments where signal propagation suffers from severe multipath effects. In addition, automatic power adjustment strategy commonly implemented in modern APs, which monitors surrounding channel conditions and accordingly optimizes the transmitting power, further exaggerates the RSS temporal fluctuations. Device heterogeneity also results in diverse RSS measurements on different devices. Such RSS variations lead to significant impacts of RSS fingerprints including (1) *spatial ambiguity*: fingerprints from different individual locations appear to be similar and thus indistinguishable from each other, giving rise to fingerprint mismatches and therefore inducing notable location errors; and (2) *temporal instability*: fingerprint observations at a specific location would vary over time, making them deviate from and therefore fail to match the one collected during the training phase. Both issues would hurt the location accuracy and reside as two long-standing yet inevitable problems of RSS fingerprinting.

To overcome spatial ambiguity, additional information like digital floorplan [20], acoustic ranging [22], image matching [42] and inertial sensing [14, 32] have been recently incorporated with RSS fingerprinting for improved performance. While these approaches achieved better accuracy, they also degraded the delightful ubiquity and induce additional costs of RSS fingerprinting systems. For example, users need to intentionally take pictures [42] or cooperate with multiple peers [22] for localization. Considering temporal instability, the fingerprint database may need to be periodically calibrated, either reconstructed or updated to adapt to RSS variations [19, 37, 46]; Otherwise an initial fingerprint database may gradually deteriorate, leading to grossly inaccurate location estimations. Although crowdsourcing-based approaches reduce the efforts of fingerprint database construction [28] and adaptation [37], the adaptation costs are still non-negligible and they cannot adapt to transient RSS variations due to limited execution frequency. Since spatial ambiguity and temporal instability arise from the inherent properties of RSS fingerprint, physical layer Channel State Information (CSI) is recently exploited for precise localization [18, 29, 33]. The CSI is only available on specific WiFi devices with slight driver modifications and is not accessible on commodity smartphones. Hence as for practical location services, we believe new promising solutions to overcome these fundamental limitations lie in exploring new forms of fingerprints that is resistant to RSS uncertainty.

To better deal with RSS variations, we exploit the spatial feature of RSS fingerprints and propose *Fingerprint Spatial Gradient* (FSG), a new form of WiFi fingerprints that turns out to be more spatially distinctive and temporally stable. The key insight is that the spatial relationships of multiple RSS fingerprints from neighbouring

locations would be more robust than individual RSS fingerprints from one single location. The FSG profile of one location depicts the differences between its representative RSS fingerprints and those of a set of nearby locations, which would hold specific patterns subjected to the underlying spatial constraints of fingerprints from adjacent locations. For example, considering a location with its surrounding neighbours on two sides along a corridor, the resulted FSG would in principle exhibit a "V"-like pattern, regardless of their own fingerprints. As a relative form, FSG can better mitigate the impacts of variations caused by absolute AP power changes and measurement device diversity. For example, if some AP adjusts its transmission power, the RSS values perceived at multiple neighbouring locations would be all affected, thus keeping the relative FSG less changed than the absolute RSS values (although still changed). As a result, the proposed FSG is more stable and identifiable than plain RSS fingerprints as it gracefully tolerates RSS variations caused by either environmental dynamics or device diversity.

Incorporating FSG in a practical localization system, we present ViVi to interpret the construction, representation, and comparison of FSG with a full functional implementation. We first formally specify FSG with experimental validation. Then FSG profiling is conducted on top of the general RSS fingerprint database. We design novel algorithms to generate optimum FSG of each location by selecting its best nearby fingerprints for FSG profiling. Finally, we propose proper FSG matching measures to compare two FSG profiles for effective location estimation. The design of ViVi follows the classical fingerprinting framework. Its inputs are no more than any traditional RSS fingerprint based systems. Thanks to the superior FSG, ViVi effectively remedies the spatial ambiguity and temporal instability of RSS fingerprints and achieve performance gain without the pains of introducing any extra information (e.g., inertial sensor hints [14], acoustic ranging [22]) or additional service restrictions (e.g., peer cooperation [22], taking images [42], monitoring trajectory [45]) or making strict assumptions on RSS models [38].

To validate the effectiveness and performance of ViVi, we conduct experiments in different buildings. The results demonstrate that ViVi achieves great performance, with a mean accuracy of 3.2m and a 95th percentile accuracy of 6.4m, outperforming the best among four comparative approaches by >28% and >19% and exceeding the worst comparative case by 38.5% and 23.8%, respectively. We envision FSG as an effective supplement and alternative to existing RSS fingerprints that sheds a light on practical WiFi-based localization in the future.

In summary, the core contributions are as follows.

(1) Based on in-depth understanding of RSS fingerprints, we propose a novel form termed as *fingerprint spatial gradient*, which is built upon RSS fingerprints and exploits the underlying spatial properties of nearby fingerprints and turns out to be more stable and distinctive than the original RSS fingerprints.
(2) We propose novel algorithms to construct effective FSG profiles based upon a common RSS fingerprint database and design efficient FSG matching methods for location estimation. The resulted system ViVi well overcomes the drawbacks of spatial ambiguity and temporal instability adhering to previous RSS fingerprints.
(3) We prototype ViVi on smartphones and conduct extensive experiments in different buildings with the implementation of four different start-of-the-art approaches as comparison. The results demonstrate ViVi achieves remarkable performance gain without the pains of resorting to additional information or restrictions or impractical model assumptions.

The rest of the paper is organized as follows. Following an overview in Section 2, we define the concept of FSG in Section 3 and present the FSG specification, construction and comparison in Section 4. We implement and evaluate ViVi in Section 5. We review the start-of-the-art in Section 6 and conclude this work in Section 7.

2 VIVI DESIGN

Before we present the architecture of ViVi, we first review and summarize the typical framework of fingerprint-based localization.

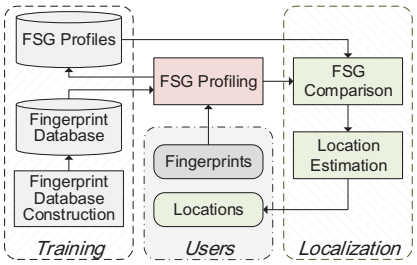

Fig. 1. Overview of ViVi flow

The mainstream of existing fingerprint-based approaches employ RSS observations at one location as its fingerprints. Such systems typically consist of two phases: An RSS fingerprint database is constructed a prior during an *offline training phase*. Location is then estimated via fingerprint matching during the *online localization phase*. Such scheme is widely adopted for smartphone localization due to the ubiquitous availability of WiFi infrastructure [20, 22, 28, 43, 44].

Formally, the area of interests is sampled as a discrete location space $\boldsymbol{L} = \{\boldsymbol{l}_1, \boldsymbol{l}_2, \cdots, \boldsymbol{l}_n\}$ where n is the amount of sample locations. For each location $\boldsymbol{l}_i$ with coordinates (x_i, y_i), a corresponding fingerprint is denoted as $\boldsymbol{f}_i = \{f_{i1}, f_{i2}, \cdots, f_{im}\}$, $1 \le j \le m$, where f_{ij} denotes the RSS value (or the RSS distribution in probabilistic algorithms [47]) of the jth AP and m is the total number of APs in the targeted location space. All fingerprints form a fingerprint space $\boldsymbol{F} = \{\boldsymbol{f}_1, \boldsymbol{f}_2, \cdots, \boldsymbol{f}_n\}$, corresponding to the location space $\boldsymbol{L}$. The radio map consisted of $< \boldsymbol{l}_i, \boldsymbol{f}_i >$ terms is usually constructed either manually by site survey or automatically by crowdsourcing [28, 43]. Then location estimation is conducted by retrieving the best match of a query fingerprint against the whole fingerprint space $\boldsymbol{F}$, using some specific fingerprint similarity measures such as Euclidean distance.

In principle, there are two major issues of fingerprint-based localization, i.e., fingerprint database construction and location accuracy. The former is an annoying task that is previously accomplished by manual site survey. Fortunately, it has been largely automated and eased by recent crowdsourcing-based techniques [1, 28, 30, 34, 43]. In this paper, we mainly focus on the later issue to achieve higher accuracy for practical applications.

Now we present the overall logic flow of ViVi, an accurate and robust indoor localization based on fingerprint spatial gradient. As shown in Fig. 1, the design of ViVi follows a classical fingerprinting scheme in consideration of compatibility with existing approaches. Its inputs are no more than any typical RSS fingerprint based localization systems. The core contributions lie in the introduction of an FSG profiling module along with an FSG comparison module.

Specifically, during the training phase, we additionally perform an *FSG profiling* procedure to build the FSG profiles for all sampling locations on top of the traditional fingerprint database. In the localization stage, when matching a user query $\boldsymbol{f}_Q$ against one candidate sampling location $\boldsymbol{l}_C$, we construct a querying FSG profile $g_{Q(C)}$ tailored to this candidate location based on information of its specific FSG g_C (i.e., the selected nearby locations and corresponding fingerprints). Then we compute the similarity of the two FSG profiles, denoted as $\Gamma(g_{Q(C)}, g_C)$, in the *FSG comparison* module. We employ FSG matching paradigm, instead of a model fitting approach, in purpose of avoiding fragile assumptions on a theoretical FSG model that is vulnerable to practical noises. Thus the final location estimate for a query $\boldsymbol{f}_Q$ is output by *location estimation* module as the candidate location that reports the minimal FSG dissimilarity (We denote $g_{Q(C)}$ as g_Q for sake of simplicity hereafter):

$$\boldsymbol{l}_Q^* = \arg\min_{\boldsymbol{l}_C \in \boldsymbol{L}} \Gamma(g_Q, g_C). \tag{1}$$

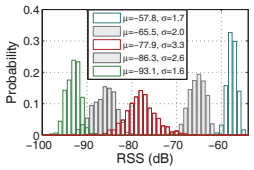

Fig. 2. RSS bias over time

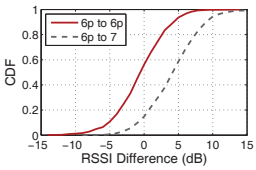

Fig. 3. RSS bias over different devices

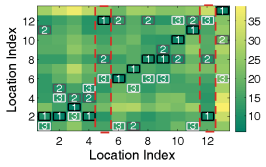

Fig. 4. Fingerprint spatial ambiguity

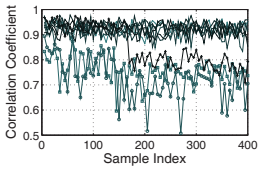

Fig. 5. Fingerprint temporal instability

ViVi is also implemented with an AP selection procedure to filter out low quality APs, especially those have extremely low mean RSSs or suffer from significantly high variances at the same location. To further reduce the computation costs, in practice we do not need to consider every sample location, but can efficiently skip those candidates that share too few common APs to reduce the search space.

The proposed ViVi is computation efficient. The only relatively complex FSG profiling procedure is conducted during the offline training phase. And once the FSG profile for each sample location is constructed, it does not need to be recalculated in the future, unless the fingerprint database is reconstructed or adapted. During the online localization, the only extra computation costs, compared to traditional RSS fingerprint-based approaches, lie in the FSG construction for each comparison, which can be fortunately computed in constant time, given that the FSG profile of the candidate location is available.

In the following, we first present the specification and advantages of the proposed FSG and then introduce how to profile and compare them.

3 UNDERSTANDING FINGERPRINT SPATIAL GRADIENT

3.1 Limitations of Existing RSS Fingerprints

Despite of various innovations that have been proposed to ease the fingerprint construction [16, 28, 30, 34] or advance the fingerprint matching [13, 20, 22, 45] in purpose of promoting practical applications, existing RSS fingerprints suffer from several critical limitations due to especially the RSS variations.

RSS is known to be vulnerable to uncertain environmental dynamics and sensitive to hardware models [20, 37, 47]. As shown in Fig. 2, we collect about 1500 RSS samples of different APs and illustrate the RSS distributions of 5 APs with diverse average RSS values. Apparently, such variations cannot be trivially alleviated by cutting off the APs with low RSSs [4, 9] because, as shown in Fig. 2, stronger APs do not necessarily suffer smaller variations in RSS. One major cause of such RSS temporal fluctuations is the uncertain dynamics of indoor environments, including instantaneous interferences from human movements and door opening/closing and prolonged changes of temperature, humidity, as well as AP transmission power. Device heterogeneity is another well-known factor that leads to RSS bias [6]. Due to inherent hardware characteristics, different devices may encounter diverse RSSs of a specific AP under even identical wireless conditions. For example, we measure RSSs at 50 different locations using three devices of two different models (two Google Nexus 6p phones and a Nexus 7 phone) simultaneously and compare the differences in Fig. 3, which clearly demonstrates the RSS biases of different phones. As seen, even two smartphones of the same model (e.g., the results of two Google Nexus 6p phones) suffer from non-negligible RSS differences.

Evidently, RSS variations may induce two aspects of severe influences, i.e., spatial ambiguity and temporal instability, as also observed and recognized by previous works [6, 22, 47]. We explain the impacts of them concretely with real measurement data as follows.

(1) *Spatial ambiguity*: One fingerprint might be similar to those from two or more (even quite distant) locations, rendering fingerprints over different locations become indistinguishable. Fig. 4 shows the similarity matrix of fingerprints from 13 locations in corridors, where the three most similar fingerprints

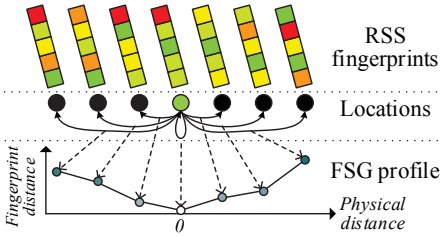

Fig. 6. Illustration of FSG profile (of the central green sample location)

in each column with the one on the diagonal line are marked by "1" in black box, "2" in gray box and "3" in white box in sequence. As seen, the most similar fingerprints do not always come from the same nor even close locations. Such phenomenon is recognized as spatial ambiguity that introduces significant fingerprint mismatches [22, 42].

(2) *Temporal instability*: The fingerprint of a location observed at one instant does not match the initially collected training fingerprints from the same location. As shown in Fig. 5, although the fingerprints of some locations are relatively stable, the temporal correlations between a sequence of fingerprints successively measured at some other locations may notably decrease with respect to time. Consequently, fingerprints from the same or close locations cannot be successfully matched.Furthermore, severe temporal instability would degrade the performance of originally constructed fingerprint database especially over long-term running [37].

To conclude, both issues can lead to severe fingerprint mismatches and thus impair the localization accuracy and reside as two long-standing yet inevitable problems of conventional RSS fingerprints. The problem, however, is non-trivial and could not be fully addressed by simply applying an outlier detection techniques or increasing AP number. Different approaches have been proposed to deal with the two issues from various perspectives. Early efforts like Horus [47] employ advanced probabilistic models to tolerate RSS variations. Recently, stimulated by mobile phone development, various sensor information are incorporated to enable improved localization, including acoustic ranging [22, 26], image matching [42, 48], inertial sensors [28, 30, 34, 43, 45], etc. All these approaches, as far as we are aware of, are designed with RSS fingerprint as the basic form for location fingerprints. In contrast, we explore and exploit a new form for WiFi fingerprinting by leveraging the spatial gradient of RSS fingerprints. Hence our approach is orthogonal and compatible to existing systems. Several latest innovations [30, 31, 48] also leverage spatial features of RSS, yet in a different manner, as detailed in the next section.

3.2 Fingerprint Spatial Gradient

Instead of using the RSS fingerprints, we propose FSG to exploit the spatial feature of fingerprints from multiple adjacent locations. The key insight is that certain spatial relationship among multiple adjacent locations' fingerprints keeps relatively stable against signal variations, although their individual fingerprint might be altered. Specifically, fingerprints collected from closer locations are generally more similar to each other, while distant locations enjoy larger fingerprint differences. Note that we do not assume that every pair of neighbouring fingerprints are similar. Indeed there would be some locations that occasionally hold widely different fingerprints with their neighbours (as shown in Fig. 4). Nevertheless, it is promisingly feasible to seek for a set of neighbouring locations among all that hold reasonable and stable fingerprint similarity relationships, even if some of them might suffer from spatial ambiguity. For a specific location, such spatial trend of fingerprint similarity is expected to be stabler than an individual fingerprint of its own. Benefiting multiple fingerprints across different spatial locations, the resulted profiles also would be more distinguishable than a single RSS fingerprint. Hence we explore

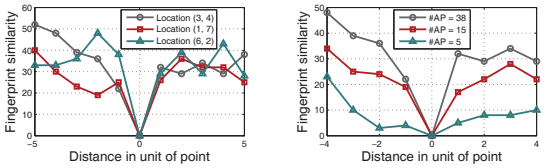

(a) Different locations (b) Different AP number

Fig. 7. FSG profiles by experimental measurements

and exploit such fingerprint spatial gradient as a more favorable feature, compared with the widely adopted original RSS fingerprints, for location mapping.

3.2.1 FSG Specification. As shown in Fig. 6, for a specific location, the FSG profile describes the fingerprint similarity trend between the fingerprint of that location and several of its neighbouring locations. Specifically, the FSG profile for a location $\boldsymbol{l}_i$ is defined as

$$g_i = \{< d(\boldsymbol{l}_i, \boldsymbol{l}_j), \phi(\boldsymbol{f}_i, \boldsymbol{f}_j) >, i - r \leq j \leq i + r\}, \tag{2}$$

where $\phi(\boldsymbol{f}_i, \boldsymbol{f}_j)$ is the similarity of $\boldsymbol{f}_i$ and $\boldsymbol{f}_j$ and each $\boldsymbol{f}_j$ denotes the RSS fingerprint of one of the neighbouring locations $\boldsymbol{l}_j$. $d(\boldsymbol{l}_i, \boldsymbol{l}_j)$ denotes the physical distance between $\boldsymbol{l}_i$ and $\boldsymbol{l}_j$. Locations $\boldsymbol{l}_{i-1}$ to $\boldsymbol{l}_{i-r}$ and $\boldsymbol{l}_{i+1}$ to $\boldsymbol{l}_{i+r}$ should appear in the surrounding subspace of $\boldsymbol{l}_i$ respectively and are ordered in physical distance to the current location $\boldsymbol{l}_i$. Theoretically the FSG profile exhibits a "V"-like shape as the fingerprint similarity would first decrease to zero (at the current location) and then increase, corresponding to the ordered physical distances to the current location, which will be confirmed by the following experimental observations.

Here various similarity measures can be leveraged as the fingerprint similarity ϕ, such as Euclidean distance [3] and its temporal weighted version [11], probabilistic likelihood [47], and Kullback-Leibler Divergence [25], etc. For simplicity, we first adopt the most common p-norm distance with $p = 2$ as follows and then examine the performance of different metrics in Section 5.

$$\phi(\boldsymbol{f}_i, \boldsymbol{f}_j) = (\sum_{k=1}^{m} |f_{ik} - f_{jk}|^p)^{1/p}. \tag{3}$$

We preliminarily analyze the FSG feature through real-world experimental measurements based on a sample fingerprint database of a campus building by site survey. We first plot the FSG profile of randomly selected locations in Fig. 7a, which confirm specific spatial trends of FSG profiles at different locations. Fig. 7b further demonstrates the FSG profiles when using different number of APs in the RSS fingerprints.

Note we illustrate the "V"-like shape of FSG profiles only for intuitive conceptualization and easy understanding here. As would be explained in Section 4, our ViVi design will not require a theoretical "V" shapes (nor any other specific shapes) of FSG profiles for localization because any assumed shapes might be distorted and no longer hold as expected in practice. Instead, our design seeks for the most stable FSG profile as fingerprints.

3.2.2 FSG Advantages. The proposed FSG appears to be more temporally stable and spatially distinctive for localization than existing RSS fingerprints.

On one hand, FSG exploits the spatial constraints among multiple fingerprints from a set of elected multiple nearby locations and thus turns out to be more stable over time than RSS fingerprints that consist of absolute RSS values observed at a single location. The rationale is that certain spatial neighbouring relationships would be more stable than individual RSS fingerprints [13, 37].

On the other hand, FSG also serves more distinctively in space, although the FSG profiles themselves of different reference locations actually appear to be pretty similar (as the "V"-like patterns shown in Fig. 7a). The trick lies in that we generate the FSG of a query according to the profiled neighbouring locations of a reference location when evaluating its probability as the targeted location for this query. In other words, the querying FSG profiles are also constructed based upon the elected neighbouring fingerprints already in the fingerprint database. In addition, a query does not hold a fixed FSG profile, which inversely adapt to each different reference location when matching against it. As a result, if the query fingerprint indeed comes from the same location with the reference one, the generated querying FSG profile tend to be similar with the reference one. Otherwise, if the fingerprint is from a different location, the resulted FSG profile will exhibit significantly different spatial pattern. This is because the query fingerprint does not necessarily hold similar gradients with the reference location's neighouring fingerprints even if it itself is similar to the reference fingerprint (Two fingerprints that are both similar to a third one are not necessarily similar to each other).

Some previous works have leveraged related features of RSS spatial distribution of individual APs [16, 30, 37]. For example, GIFT [31] employs a binary differential RSS value of two adjacent locations as a replacement of the absolute RSSs. Walkie-Markie [30] and Travi-Navi [48] both observe that the spatial-temporal RSS sequence of a certain AP along a path will exhibit a specific trend from increasing to decreasing. While these works pioneer to leverage spatial features, most of them focus on different targets such as floorplan generation [30], self-navigation [48], and radio map adaptation [37]. Furthermore, all of existing approaches rely on mobile trajectories to extract *path-centered* spatial features of RSS, which usually requires dead-reckoned traces from users and is not feasible for the widely adopted point-based fingerprinting systems. In this work, we investigate the spatial gradient of nearby locations from a perspective of entire fingerprint and devise a more stable and distinguishable form of WiFi fingerprints. Our design exploits *reference-point-centered* spatial features (both the querying and reference FSG profiles are generated based on the nearby fingerprints of a referent point, see Section 4), which is fully compatible to existing fingerprint-based systems and does not resort to mobile trajectories for either fingerprint database construction or location query.

The above superior properties lay solid foundation for location distinction. In the following, we design and implement a full functional localization system based on the proposed FSG. Unless otherwise mentioned, we still refer fingerprints to traditional RSS fingerprint in the following.

4 EXPLOITING FINGERPRINT SPATIAL GRADIENT

4.1 Profiling Fingerprint Spatial Gradient

FSG profile for each reference location is built upon the original RSS radio map. There are generally multiple neighboring fingerprints for each location. Thus in this section, we first discuss how to form a good FSG profile for each reference location, e.g., how to find a representative set of neighbouring locations and how to appropriately order them. Then we present how to profile a query fingerprint based on a reference location's FSG.

4.1.1 Profiling a Reference Location. For a targeted location $\boldsymbol{l}_i$ with a fingerprint $\boldsymbol{f}_i$, we first form a neighbouring set containing all adjacent locations whose distances to the current location are no more than r sample points. Then we calculate the RSS fingerprint similarity between $\boldsymbol{l}_i$ and locations in the neighbouring set. By default, we adopt the most common Euclidean distance to measure fingerprint similarity. Nevertheless, various fingerprint similarity metrics such as other p-norm distances and Kullback-Leibler divergence can be leveraged, which will be implemented and evaluated in the experiments in Section 5. Afterwards, we propose different methods to generate an appropriate FSG profile for the current location $\boldsymbol{l}_i$: two heuristics based on spatial gradients and one considering temporal variances of spatial gradients.

(1) Minimizing Local Gradient. As shown in Fig. 8a, the basic idea of minimizing local gradient (MinLG) is to select the next neighbouring location in a greedy way. Starting from $\boldsymbol{l}_i$, we choose the top two adjacent

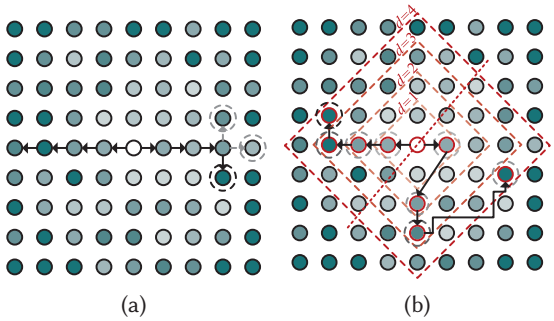

Fig. 8. Illustration of FSG profiling by (a) Minimizing Local Gradient and (b) Maximizing Global Gradient. Circles with darker color indicate larger fingerprint distances (gradient) to the targeted point marked by empty circles.

locations that have the smallest fingerprint distances as the two expanding direction. The rationale is that two adjacent locations are more common to share more similar fingerprints. For each following step, we select the location (among all unselected adjacent locations within one-sample-point distance with the current selected location) that yields the shortest fingerprint distance with the current location. We repeat doing this until we gain r locations on each direction. After that, we order the respective set of r neighbouring locations on each direction by physical distance to $\boldsymbol{l}_i$ and, together with the fingerprint distances, forming an FSG profile of $\boldsymbol{l}_i$. The complexity of of profiling one sample location by MinLG is $O(6r + 4)$ since fingerprint gradients of three additional neighbours need to be calculated for each of the $2r$ selected candidates.

(2) Maximizing Global Gradient. An alternative method opts for the top $2r$ neighbours that share the largest fingerprint distances with the targeted location $\boldsymbol{l}_i$ to maximize the global gradient (MaxGG) of the resulted FSG.

To achieve this, we first calculate the fingerprint similarity between $\boldsymbol{f}_i$ and the representative fingerprint of each neighbouring location. As shown in Fig. 8b, we increase the distance constraints d to the target point step by step and select two most dissimilar fingerprints for each step. By doing this, we obtain $2r$ neighbouring points when the distance increases to r sample points. To gain identical number of points on either size of the current locations, we search for a division that passes through the current location in the physical space and cuts the $2r$ locations into two equal parts. Then we connect the locations in each part in the order of physical distances to the current location, resulting in a legitimate FSG profile. The complexity of profiling one sample location using this MaxGG algorithm is $O(N_r)$ where N_r is the number of neighbouring sampling locations within the range r of $\boldsymbol{l}_i$. Considering the squared sample grid as illustrated in Fig. 8b, the complexity becomes $O(\frac{4}{3}(4^r - 1))$.

(3) Optimizing Spatial Stability. The above two heuristic approaches are efficient but, however, does not necessarily guarantee the best profiles. Recalling that the key insight of FSG is to exploit spatial fingerprint relationships that are stable over time, we propose another algorithm for FSG profiling by choosing a set of neighbouring fingerprints that optimize the spatial stability (OptSS) in terms of fingerprint similarity.

In general, when we mention the (representative) fingerprint of one location, we commonly refer to the averaged vector of multiple raw fingerprints from that location [22, 42, 43, 47]. Different from the above two approaches, we leverage every single fingerprint record here, instead of the averaged one, to output an optimal set of neighbouring fingerprints. We first compute the fingerprint distance between the representative fingerprint $\boldsymbol{f}_i$ of target location $\boldsymbol{l}_i$ and every raw fingerprint record of each neighbouring candidate. Then we derive the variances of the resulted fingerprint distances for each neighbour and form a variance matrix. Take Fig. 8b as a substitutive illustration and imagine the color of each location indicates the variance of corresponding fingerprint distances. We select two neighbouring locations that have the smallest variances for each step of physical distance d and obtain $2r$ neighbours in total. After that we generate the FSG of current location $\boldsymbol{l}_i$ by dividing the selected

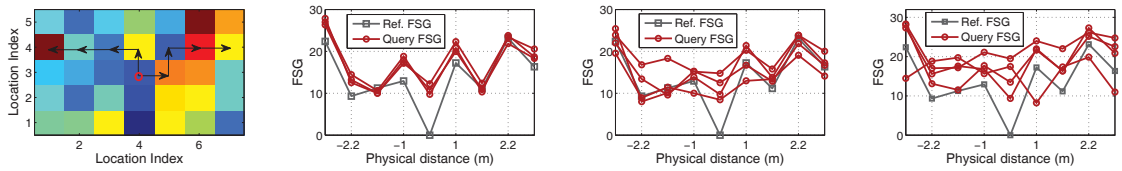

Fig. 9. FSG profile comparison: (a) Reference FSG profiling by minimizing local gradient. FSG comparison against queries from (b) the same location, (c) 1-meter neighbour locations, (d) 2-meter neighbour locations

neighbours into two parts with identical sizes and connecting them in order of physical distances to $\boldsymbol{l}_i$. By doing this, the acquired FSG is optimized in spatial stability since we always select the spatial neighbours that output the most stable relationships (i.e., minimized variances in fingerprint distances). The complexity of profiling each sample location is $O(N_r(m+1))$, where N_r is the number of neighbouring sampling locations within the range r and m is the number of raw fingerprint records of each sample location. Taking the grid topology in Fig. 8b as example, the complexity is $O(\frac{4}{3}(4^r-1)(m+1))$. Considering that r is generally a small constant number (e.g., <5), the complexity is then linear to m.

4.1.2 Profiling a Query Fingerprint. The above FSG profiling task is completed in the offline training phase, based upon an ordinary radio map. In the online localization phase, the FSG profile of a query fingerprint is not fixed and depends on the specific targeted reference point. When comparing a query fingerprint $\boldsymbol{f}_Q$ from an unknown location $\boldsymbol{l}_Q$ against a specific candidate reference location $\boldsymbol{l}_C$, we construct a FSG profile for the query using the selected neighbours in the FSG profile of $\boldsymbol{l}_C$. For example, if the FSG profile of the candidate $\boldsymbol{l}_C$ is $g_C = \{< d(\boldsymbol{l}_C, \boldsymbol{l}_j), \phi(\boldsymbol{f}_C, \boldsymbol{f}_j) >, j \in N(\boldsymbol{l}_C)\}$, then the FSG for the query turns out to be $g_Q = \{< d(\boldsymbol{l}_C, \boldsymbol{l}_j), \phi(\boldsymbol{f}_Q, \boldsymbol{f}_j) >, j \in N(\boldsymbol{l}_C)\}$. Note that beside the neighbouring point set $N(\boldsymbol{l}_C)$, we also substitute the candidate location coordinates into the query location for FSG profiling. Provided the reference FSG profile, each query FSG profile can be generated in *constant time* without the need of searching for spatial neighbours.

The key advantage by doing so is that when the query fingerprint comes from the same location with the reference one, the generated FSG profiles tend to be similar. In contrast, if the fingerprint is from a different location, the FSG profiles will be significantly different since the constructed query FSG profile does not exhibit similar spatial patterns. Take Fig. 9 as an example where $r = 4$ and consider the FSG of the location marked by a red circle in Fig. 9a. As in Fig. 9b, when comparing with different queries collected from the same locations, the generated querying FSG profiles appear to be consistently similar to the reference one. In contrast, as indicated by Fig. 9c, different patterns appear in the FSG profiles of queries from neighbouring locations only 1-meter away. Such chaotic differences are further significantly aggravated when matching queries from locations that are 2-meter away, as shown in Fig. 9d.

In addition, the FSG construction strategy also enables us to deal with any single querying fingerprint. This advances many previous approaches that usually require continuous observations along a moving trace with well-monitored inertial sensor hints [30, 31, 45] or resort to information from multiple participatory users [22]. Given the querying and training FSG profiles available, we next discuss how to compare them and further derive the best-matched location candidate.

4.2 Comparing Fingerprint Spatial Gradient

Fingerprint-based location determination problem is in principle a pattern matching problem, regardless of the specific feature used. Although the FSG normally exhibits specific "V"-like pattern, we employ a pattern matching approach for location estimation, instead of building and fitting a theoretical pattern model, because the "V"-like

pattern would be distorted in practice. By FSG matching, we avoid making fragile assumptions on the spatial gradient distribution and gain robustness to uncertain disturbances in FSG profiling in practice.

A FSG profile can be viewed as a point set in the space when treating the physical distance as X-coordinate and the fingerprint distance as Y-coordinate for each neighbour. Let $\boldsymbol{f}_Q$ be the query RSS fingerprint, and let $\boldsymbol{l}_C$ be the current candidate location. As mentioned above, we can obtain the query pattern (FSG profile) as $g_Q = \{< \boldsymbol{d}_Q, \boldsymbol{\phi}_Q >\}$ and the targeted pattern as $g_C = \{< \boldsymbol{d}_C, \boldsymbol{\phi}_C >\}$, where both patterns are $2r + 1$ point sets. Comparison of two FSG profiles can thus be solved by shape matching techniques, of which an effective similarity measure acts as the core. While Euclidean distance is widely used as a similarity metric for traditional RSS fingerprints, we need to develop effective similarity measure for the proposed FSG profile. Our goal is to explore proper similarity measures to recognize the FSG profiles from the same locations while differentiating those of different locations.

4.2.1 Cosine Similarity. As noticed, the X-coordinates of each pair of g_Q and g_C are the same. Thus we can omit the X-coordinates and apply the well-known cosine similarity on only the $\boldsymbol{\phi}$ parts. Let Γ be the similarity of two FSG profiles, we have

$$\Gamma(g_Q, g_C) = \frac{\boldsymbol{\phi}_Q \cdot \boldsymbol{\phi}_C}{||\boldsymbol{\phi}_Q||||\boldsymbol{\phi}_C||}. \tag{4}$$

4.2.2 Turning Function Distance. The turning function, or cumulative angle function, $\Theta_s(P)$ of a polyline (or polygon) P depicts the counter-clockwise angle between tangent of each segment and the X-axis as a function the edge length s. $\Theta_s(P)$ starts from a certain point on P and tracks each turning angle that appears. The turning function increases with left hand turns and decreases with clockwise turns.

An FSG profile can be translated into a polyline by connecting each two adjacent points. Thus we can derive the turning function of g_Q and g_C as $\Theta_s(g_Q)$ and $\Theta_s(g_C)$, respectively. Applying L_p Distance to the two turning functions, a dissimilarity measure on g_Q and g_C is given as:

$$\Gamma(g_Q, g_C) = \left(\int |\Theta_s(g_Q) - \Theta_s(g_C)|^p ds \right)^{1/p}. \tag{5}$$

4.2.3 Discrete Fréchet Distance. The Fréchet distance is a popular measure between parametric curves that takes into account the location and ordering of the points. It is intuitively explained by a common analogy of "dog-walking distance": A person and a dog connected by a leash are walking along two curves (without backtracking) respectively. The shortest length of the leash that is required for traversing the two curves is the Fréchet distance.

The Fréchet distance usually appears in its continuous form for parametric curves. Since we have identical constant points in both FSG profiles g_Q and g_C, the discrete version is preferred, which can be solved more efficiently in polynomial time by using dynamic programming:

$$\Gamma(g_Q, g_C) = \min_{\delta, \beta:[1:n]\to[1:n]} \max_{s\in[1:n]} \left\{ d\Big(g_Q\big(\delta(s)\big), g_C\big(\beta(s)\big) \Big) \right\}, \tag{6}$$

where $d\big(g_Q(\delta(s)), g_C(\beta(s))\big)$ denotes the Euclidean distance between the two points, δ and β range over all discrete non-decreasing surjections of the form $[1 : n] \to [1 : n]$.

Different from traditional RSS fingerprint, the proposed FSG is a *relative* spatial feature. Thus pattern matching upon FSG profiles appears to be less susceptible to signal variations caused by temporal changes or device heterogeneity, no matter what similarity measure mentioned above is used.

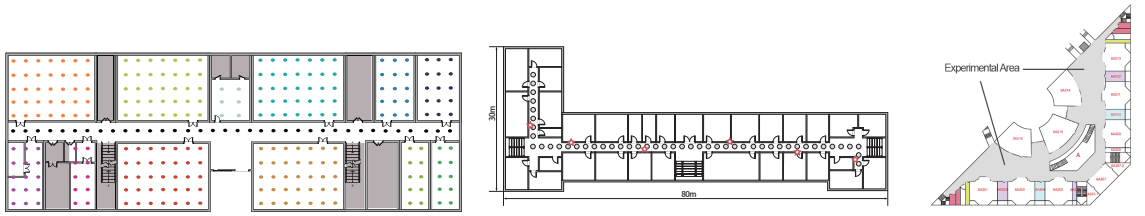

(a) Office building (b) Academic building (c) Classroom building

Fig. 10. Experimental areas

Table 1. Data collection in different scenarios

#	Building type (Areas)	Size(m^2)	Density	Devices	#Samples	#Loc	Duration
1	Academic (Public areas)	600	1m×1m	Nexus 5/7, two Nexus 6p	23.4K	93	10h in 1 day
2	Office (Whole floor)	1,500	2m×2m	Two Nexus S	27.2K	293	24h in 2 days
3	Classroom (Public areas)	3,360	1.2m×1.2m	Nexus 7, two Nexus 6p	87.0K	460	12h in 1 day

5 IMPLEMENTATIONS AND EVALUATION

We prototype ViVi on the popular Android OS and conduct experiments using different devices over various scenarios. In this section, we first introduce the experimental settings and then present the detailed evaluation.

5.1 Experimental Methodology

5.1.1 Experimental Scenarios. We carry out experiments in three buildings with different floor layouts and diverse wireless environments. Fig. 10 shows the floor plans of different experimental areas. Although the three buildings are similar on building structure, the user behavior patterns are pretty different. For example, there are many people in the office building in daytime, which will be almost empty in the night. The classroom building are crowded or empty to different extents depending on the course schedule. While there are a reasonable number of users in the academic building most of the time.

The data collection details are summarized in Table 1. When collecting fingerprints for training, we employ a typical sampling frequency of around 1Hz. We employ six phones of four different models that are manufactured by different companies for data collection, including two Samsung Nexus S, one LG Nexus 5, two HUAWEI Nexus 6p and one ASUS Nexus 7 pad, which are equipped with different types of WiFi chips.

5.1.2 Comparative Methods. To extensively evaluate the performance of ViVi, we additionally implement four different start-of-the-art approaches for comparison, which have been proposed to enhance the primary RSS fingerprinting.

1) **Horus (Probabilistic Method)** [47]: A classical probabilistic algorithm that computes the probability distribution of the RSS values at each location as the fingerprint metric, and retrieves the targets of the maximum likelihood as estimated locations.

2) **TW-KNN (Temporally Weighted KNN)** [11]: It forms fingerprints with temporally weighted RSS by applying an iterative recursive weighted average filter on training RSS samples.

3) **KLDiv (Kullback-Leibler Divergence)** [25]: A typical KNN-based localization scheme built upon RSS fingerprints, but using the Kullback-Leibler divergence of two signal distributions as the similarity measure.

4) **GIFT** [31]: A metric of binary differential value between RSSs observed at two adjacent locations is exploited as replacements to the original RSS values as fingerprints. As GIFT is designed for mobile traces, we combine queries from two adjacent locations as one for GIFT.

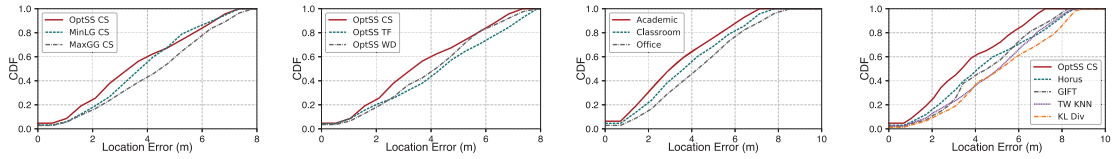

(a) Three profiling methods (b) Three FSG similarity (c) Different areas (d) Performance comparison

Fig. 11. Overall performance

We mainly aim to validate the advantages of the proposed FSG over RSS fingerprints. In other words, we focus on the relative accuracy improvement rather than the absolute accuracy achieved by ViVi. Hence we mainly implement the core fingerprinting and matching components of the above systems. For example, we omit the clustering step in Horus [47] and the Particle Filter enhancement of GIFT [31] since similar components could also be incorporated in ViVi. By default, we conduct identical preprocessing (e.g., AP selection) for all methods and implement all of them with KNN with $k = 3$. We mainly focus on the average location errors and the 95th percentile errors as performance metrics for evaluation.

5.2 Performance Evaluation

We first explore the best FSG profiling approach and the best FSG similarity metric. We integrate the results of different phones from all experimental areas for evaluation. We first use Euclidean distance as the RSS fingerprint similarity for FSG generation and will later improve with different metrics for better accuracy. As shown in Fig. 11a, OptSS achieves the best accuracy among the three profiling methods, yielding an average accuracy of 3.5 meters and the maximum error of 6.7 meters. Using OptSS as the profiling method, we compare the performance with different similarity measures for FSG comparison. As depicted in Fig. 11b, Cosine Similarity (CS) produces slight gains in both average accuracy and 95th percentile accuracy than the other two metrics, i.e., turning function distance (TF) and walking dog distance (WD). To conclude, the combination of OptSS and CS yields the best performance with mean accuracy of 3.6m and 95th percentile error of 6.7m, when using Euclidean distance for FSG generation. In the following, we use this setting by default, together with $r = 4$ and AP number of 15.

5.2.1 Performance in different areas. We evaluate the performance in three different experimental floors as illustrated in Table 1, including a small academic building, a middle office building and a large classroom building with middle. Fig. 11c shows the performance of ViVi in different areas. As seen, ViVi yields an average accuracy of 3.3m in the academic building, 4.3m in the office building and 3.8m in the classroom building. The corresponding 95th percentile location errors in these three buildings are 6.5m, 7.7m, and 7.1m respectively. The results also demonstrate that denser sample locations in smaller areas yield better accuracy, which confirms with various previous works [28, 43].

5.2.2 Performance comparison. Fig. 11d depicts the performance of the proposed ViVi as well as the four comparative approaches. As shown, ViVi achieves the best performance among all comparative systems. The average accuracy outperforms Horus by 18.2%, GIFT by about 21.7% and exceeds TW-KNN by 25.0% and KLDiv both by 30.8%. The 95th percentile accuracy outperforms the four comparative approaches by 17.3%, 15.2%, 16.3% and 20.2%, respectively. Furthermore, as shown in Fig. 12c, when employing the TW RSS as the RSS fingerprint similarity measures during FSG generation, the performance gains in average accuracy would increase to 28.6%, 30.4%, 33.3% and 38.5% respectively and the improvements in 95th percentile errors become 21.0%, 19.0%, 20% and 23.8% respectively, achieving a mean accuracy of 3.2m and 95th percentile accuracy of 6.4m. The encouraging performance gains are achieved without introducing any extra costs (except for slightly increased computation

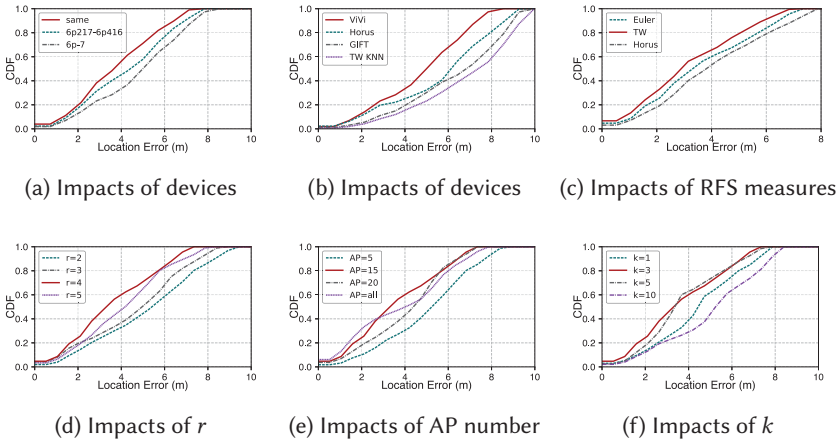

(a) Impacts of devices (b) Impacts of devices (c) Impacts of RFS measures

(d) Impacts of r (e) Impacts of AP number (f) Impacts of k

Fig. 12. Parameter study

overhead). Further improvements could be obtained by incorporating more enhanced techniques like Particle Filter, which we leave as our future work.

5.2.3 Impacts of device diversity. We evaluate the robustness of ViVi by involving diverse devices in training and querying stages. Specifically, we consider the following cases: 1) data from an identical phone for both training and testing; 2) data from one phone for training and data from another phone of the same model for testing; 3) data from phones of one model for training and data from phones of another different model for querying. As shown in Fig. 12a, device diversity indeed degrades the localization performance. The average errors increase from 3.7m (using the same phone) to 4.2m (using the same model phones) to 4.7m (using different model phones). We also test the performance of comparative methods using different devices (Nexus 6p vs Nexus 7). As shown in Fig. 12b, compared with ViVi, all comparative methods based on RSS fingerprints suffer more significantly from device heterogeneity. The mean accuracy of ViVi exceeds Horus by 17.5%, GIFT by 25.4%, and TW-KNN by 30.9%. The results demonstrate that the proposed FSG tolerate device diversity much better than RSS fingerprints.

5.2.4 Impacts of RSS fingerprint similarity (RFS) measures. As we have mentioned in Section 4, different similarity measures for RSS fingerprint comparison can be incorporated in Eqn. 3 for FSG generation. Thus we employ two additional measures that have been adopted in previous works, i.e., probabilistic likelihood (Horus) as in Horus [47] and temporally weighted Euclidean distance (TW) as in TW-KNN [11]. Fig. 12c illustrates the similar performance achieved by the above similarity measures. The results demonstrate that, although TW yields better accuracy than the other metrics, ViVi does not rely on complicated RFS measures and yields robust accuracy regarding different measures.

5.2.5 Impacts of neighbour number. In the above, we use 8 neighbours ($r = 4$) to generate FSG profiles. Now we dig into the performance of ViVi when using different numbers of neighbour fingerprints with r ranging from 2 to 5. As shown in Fig. 12d, the location errors decrease from 5.1m to 3.6m when r increases from 2 to 4 and achieves the best case at 4. The results indicate that more neighbouring locations hold more stable spatial constraints, which could not be depicted well by too few neighbouring fingerprints. However, when r further grows to 5, the performance slightly degrades to mean error of 4.1m. This is because, as r increases, fingerprints

from very distant locations will also be involved. These distant fingerprints do not contribute to, but in the contrast will impair, the stableness of the generated FSG.

5.2.6 Impacts of AP number. We examine the impacts of AP number involved in the original RSS fingerprints. We evaluated the performance using 5, 15, 20, and all APs without filtering, respectively. As shown in Fig. 12e, ViVi achieves the best performance when using 15 APs. The performance degrades with both more or less APs (e.g., the mean errors with 5 and 20 APs are 5.0m and 4.1m, larger than that with 15 APs by more than 30% and 15% respectively). The reasons are that using too few APs may loss the spatial distinctiveness of fingerprints while using too many of them will as well involve in those low quality APs. Although we filter out some apparently bad APs by signal strengths, the selected APs may not be all superior for location distinction.

5.2.7 Impacts of k. We choose $k = 3$ by default for KNN. Fig. 12f portrays the performance when using different values for k. As seen, the best results are achieved with $k = 3$, which are similar to that when $k = 5$. The location errors increase no matter larger or smaller k values are adopted since bias exist with too few candidates while too many candidates would involve low confident estimations.

5.2.8 System latency. Finally, we test the running latency of ViVi by stimulating consecutive user queries. We randomly select one query fingerprint from a set of queries and ViVi returns the location estimations. Then we average the time delays for 1000 such queries. For each comparative method, we run the same process and calculate the average running time.The average query delay of ViVi is 0.33s per query, which is similar with or shorter than previous works. As comparison, the per query delays of Horus, GIFT, and TW-KNN are 0.38s, 0.77s, and 1.04s, respectively.

5.3 Discussions

In this paper, we mainly aim to achieve better accuracy regarding temporal changes. As for long-term changes that impose severe impacts on the radio map, we believe automatic and adaptive adaptation techniques like AcMu [37] should be applied to update the fingerprint database. Yet we also plan to deploy real systems in the future and collect long-term and large-scale running data for extensive evaluation.

As we conduct experiments in public areas with existing APs, we could not intentionally control and adjust the APs for experiments. As a result, we did not explicitly provide quantitative AP power changes in the evaluation. But as we collect data in realistic environments where AP powers do change, we actually implicitly consider the power change effects and output good results regarding the changes. In the future, we intend to achieve finer-grained design of FSG to better mitigate AP power changes.

6 RELATED WORK

Indoor localization has attracted vast research efforts during the past decades. We briefly review the most related latest works in the following.

Easing Deployment. Site survey has been a major bottlenecks for fingerprint-based localization, which is time-consuming and labour-intensive. Among various research efforts, recent crowdsourcing-based approach shed promising light in easing the site survey costs [28, 34, 43]. Both [6] and [7] propose zero-calibration systems for realistic environments. OIL [27] facilitates rapid coverage by building an organic surveying system. Simultaneous Localization and Mapping (SLAM) techniques are incorporated to avoid the training costs, which result in a set of technique advancements including WiFiSLAM [10], GraphSLAM [15], and SemanticSLAM [1]. In addition to radio maps, pioneer works including [8, 16, 30] further consider automatic construction of floorplans, which also stimulates significantly the practical deployment of WiFi-based localization. Specifically, Walkie-Markie [30] exploits RSS trends along pathways for reconstruction of indoor pathways. Targeting at a

different perspective of accuracy for fingerprint-based localization, ViVi is orthogonal with these works and can be put together to enable practical indoor positioning services.

Enhanced Matching. Many efforts have been devoted to enable precise location estimation since WiFi-based indoor localization was conceptualized. Early efforts such as the well-known Horus system [47] employ advanced probabilistic methods to enhance the first fingerprinting system RADAR [3]. Various subsequent works tend to utilize complicated pattern matching techniques, investigate advanced similarity metrics, or seek for alternative expressive form of of RSS fingerprints [4, 11, 12, 20, 25]. In particular, some recent innovations also explore the spatial/temporal properties of sequential RSSs for localization. Walkie-Markie [30] is the first to explore changing trends of sequential RSSs along pathways. Similar idea is implemented in [16]. Besides both of them are designed for floorplan construction, they are only applicable for mobile trajectories. In contrast, ViVi exploit optimum spatial gradient of fingerprints among surrounding locations, rather than mobile traces, for another goal of location accuracy. WarpMap [45] defines a new type of sequence-based radio map, which replaces traditional point-based radio map, to exploit the benefits of indoor path structure. It yields delightful results for only mobile traces in constrained environments with narrow pathways. INTRI [13] combines RSS contours with traditional fingerprinting for better accuracy. To deal with device heterogeneity, RSS-Ratio [5] is proposed to model the differential RSS of RSSs on two antennas on the receiver device. However, it relies on MIMO systems and is not suitable on commodity smartphones. GIFT [31] defines a binary valued metric for differential RSS, i.e., the difference of RSSs from two adjacent locations, as a replacement of absolute RSSs to deal with signal variations. Relying on differential RSS as query inputs, GIFT can only deal with mobile traces that contain sequential RSS measurements. Differently, ViVi explores the spatial gradient of selected multiple neighbouring fingerprints and is not tied to mobile trajectories.

Sensor-assisted Enhancement. Some works resort to extra information sources beyond WiFi measurements to gain better accuracy. Ranging via acoustic signals [22] or WiFi Direct [17] among multiple devices are introduced to alleviate fingerprint ambiguity. Applying a similar idea, Argus [42] makes use of visual images to obtain extra position constraints for fingerprinting. Fusing inertial sensor data also attracts extensive studies. SurroundSense [2] integrates various sensor hints as multi-modal fingerprints for localization. More commonly, motion information is fused to provide relative locations to improve fingerprint-based localization [44]. [14] and [28] utilize geometric constraints imposed by both mobility information and digital floorplan. While remarkable accuracy is gained by these approaches, they generally rely on additional information from extra sensors, multiple devices or many participatory users. To the contrary, ViVi works merely on existing RSS measurements, achieving better accuracy without degrading the ubiquity in pervasive applications.

CSI-based Localization. Recently, the Physical layer Channel State Information (CSI) has been exposed to upper layer for high accuracy location determination. SpotFi [18] achieves decimeter-level location accuracy by accurately computing the angle of arrival (AoA) of multipath components using CSI. Chronus [33] enables a single WiFi access point to localize clients to within tens of centimeters. PinLoc [29] employs CSI as fingerprints and yield remarkable accuracy, yet with significant training costs. FILA [38] extract the direct path components with CSI for accuracy ranging. Splicer [39] derives high resolution power delay profiles by splicing the CSI measurements from multiple WiFi frequency bands. CSI is also leveraged for passive localization and tracking [21, 35]. LiFS [35] passively localizes a user with multiple links by deliberating qualified subcarriers. Dynamic-Music [21] leverages the incoherence between reflecting signal and static signal to separate reflecting signal and estimate its AoA. Despite of high precision achieved, these works rely on specialized WiFi Network Interface Cards like Intel 5300 to extract CSI, which is not available on commodity smartphones. Other systems like ArrayTrack [40] use specialized antenna arrays to track fine-grained location of wireless clients in real time. ToneTrack [41] employs frequency hopping to approach high time-of-flight resolutions for localization, yet resorts to software-defined radios.

To conclude, while most of existing approaches achieve remarkable accuracy for WiFi-based localization, they usually in the meantime introduce additional costs and constraints such as peer cooperation, mobility hints, digital floorplan information, and/or physical layer information, etc, which largely degrades the applicability and ubiquity in practice. In the contrary, our proposed approach is built upon a classical fingerprint-based framework and achieves performance gain without such pains at all, thus holding superior potentials for ubiquitous applications.

7 CONCLUSIONS

In this paper, we propose a new form of RSS fingerprint termed as fingerprint spatial gradient, which exploits the underlying spatial properties of nearby fingerprints and turns out to be more stable and distinctive than the original RSS fingerprints. On this basis, we present ViVi to incorporate the proposed FSG in a practical localization system. We first propose novel algorithms to construct FSG profiles on top of the RSS fingerprint database and design efficient FSG matching methods for location estimation. ViVi well overcomes the drawbacks of spatial ambiguity and temporal instability adhering to previous RSS fingerprints and achieves performance gain without the pains of resorting to additional information or restrictions or vulnerable RSS model assumptions. We prototype ViVi on smartphones and conduct extensive experiments in different buildings. The results demonstrate that ViVi yields great performance, outperforming start-of-the-art approaches.

ACKNOWLEDGMENTS

This work is supported in part by the NSFC under grant No. 61672319 and 61632008, 61522110 and National Key Research Plan under grant No. 2016YFC0700100.

REFERENCES

[1] H. Abdelnasser, R. Mohamed, A. Elgohary, M. F. Alzantot, H. Wang, S. Sen, R. R. Choudhury, and M. Youssef. 2016. SemanticSLAM: Using Environment Landmarks for Unsupervised Indoor Localization. *IEEE Transactions on Mobile Computing* 15, 7 (July 2016), 1770–1782.

[2] M. Azizyan, I. Constandache, and R. Roy Choudhury. 2009. Surroundsense: mobile phone localization via ambience fingerprinting. In *Proceedings of the ACM MobiCom*.

[3] P. Bahl and V. N Padmanabhan. 2000. RADAR: An in-building RF-based user location and tracking system. In *Proceedings of the IEEE INFOCOM*.

[4] Yiqiang Chen, Qiang Yang, Jie Yin, and Xiaoyong Chai. 2006. Power-efficient access-point selection for indoor location estimation. *Knowledge and Data Engineering, IEEE Transactions on* 18, 7 (2006), 877–888.

[5] W. Cheng, K. Tan, V. Omwando, J. Zhu, and P. Mohapatra. 2013. RSS-Ratio for enhancing performance of RSS-based applications. In *Proceedings of the IEEE INFOCOM*.

[6] Krishna Chintalapudi, Anand Padmanabha Iyer, and Venkata N. Padmanabhan. 2010. Indoor Localization Without the Pain. In *Proceedings of the ACM MobiCom*.

[7] Rizanne Elbakly and Moustafa Youssef. 2016. A Robust Zero-Calibration RF-based Localization System for Realistic Environments. In *Proceedings of the IEEE SECON*.

[8] A. Eleryan, M. Elsabagh, and M. Youssef. 2011. Synthetic Generation of Radio Maps for Device-Free Passive Localization. In *Proceedings of the IEEE GLOBECOM*.

[9] Shih-Hau Fang and Tsungnan Lin. 2012. Principal component localization in indoor wlan environments. *Mobile Computing, IEEE Transactions on* 11, 1 (2012), 100–110.

[10] Brian Ferris, Dieter Fox, and Neil Lawrence. 2007. WiFi-SLAM using Gaussian process latent variable models. In *Proceedings of the IJCAI*.

[11] D. Han, S. Jung, M. Lee, and G. Yoon. 2014. Building a Practical Wi-Fi-Based Indoor Navigation System. *IEEE Pervasive Computing* 13, 2 (Apr 2014), 72–79.

[12] S. He and S. H. G. Chan. 2016. Wi-Fi Fingerprint-Based Indoor Positioning: Recent Advances and Comparisons. *IEEE Communications Surveys Tutorials* 18, 1 (Firstquarter 2016), 466–490.

[13] Suining He, Tianyang Hu, and S.-H. Gary Chan. 2015. Contour-based Trilateration for Indoor Fingerprinting Localization. In *Proceedings of the ACM SenSys*.

[14] Sebastian Hilsenbeck, Dmytro Bobkov, Georg Schroth, Robert Huitl, and Eckehard Steinbach. 2014. Graph-based Data Fusion of Pedometer and WiFi Measurements for Mobile Indoor Positioning. In *Proceedings of the ACM UbiComp*.

[15] J Huang, D Millman, M Quigley, and D Stavens. 2011. Efficient, generalized indoor WiFi GraphSLAM. In *Proceedings of the IEEE International Conference on Robotics and Automation*.
[16] Yifei Jiang, Yun Xiang, Xin Pan, Kun Li, Qin Lv, Robert P. Dick, Li Shang, and Michael Hannigan. 2013. Hallway Based Automatic Indoor Floorplan Construction Using Room Fingerprints. In *Proceedings of the ACM UbiComp*.
[17] Junghyun Jun, Yu Gu, Long Cheng, Banghui Lu, Jun Sun, Ting Zhu, and Jianwei Niu. 2013. Social-Loc: Improving Indoor Localization with Social Sensing. In *Proceedings of the ACM SenSys*.
[18] Manikanta Kotaru, Kiran Joshi, Dinesh Bharadia, and Sachin Katti. 2015. SpotFi:Decimeter Level Localization Using WiFi. In *Proceedings of the ACM SIGCOMM*.
[19] Parameshwaran Krishnan, AS Krishnakumar, Wen-Hua Ju, Colin Mallows, and Sachin Ganu. 2004. A system for LEASE: Location estimation assisted by stationary emitters for indoor RF wireless networks. In *Proceedings of the IEEE INFOCOM*.
[20] Liqun Li, Guobin Shen, Chunshui Zhao, Thomas Moscibroda, Jyh-Han Lin, and Feng Zhao. 2014. Experiencing and Handling the Diversity in Data Density and Environmental Locality in an Indoor Positioning Service. In *Proceedings of the ACM MobiCom*.
[21] Xiang Li, Shengjie Li, Daqing Zhang, Jie Xiong, Yasha Wang, and Hong Mei. 2016. Dynamic-Music: accurate device-free indoor localization. In *Proceedings of ACM UbiComp*.
[22] Hongbo Liu, Yu Gan, Jie Yang, Simon Sidhom, Yan Wang, Yingying Chen, and Fan Ye. 2012. Push the limit of WiFi based localization for smartphones. In *Proceedings of the ACM MobiCom*.
[23] Kaikai Liu, Xinxin Liu, and Xiaolin Li. 2013. Guoguo: Enabling Fine-grained Indoor Localization via Smartphone. In *Proceedings of the ACM MobiSys*.
[24] Dimitrios Lymberopoulos, Jie Liu, Xue Yang, Romit Roy Choudhury, Vlado Handziski, and Souvik Sen. 2015. A Realistic Evaluation and Comparison of Indoor Location Technologies: Experiences and Lessons Learned. In *Proceedings of ACM/IEEE IPSN*.
[25] Piotr Mirowski, Philip Whiting, Harald Steck, Ravishankar Palaniappan, Michael MacDonald, Detlef Hartmann, and TinKam Ho. 2012. Probability Kernel Regression for WiFi Localisation. *Journal of Location Based Services* 6, 2 (June 2012), 81–100.
[26] Rajalakshmi Nandakumar, Krishna Kant Chintalapudi, and Venkata N. Padmanabhan. 2012. Centaur: Locating Devices in an Office Environment. In *Proceedings of the ACM MobiCom*.
[27] Jun Geun Park, Ben Charrow, Dorothy Curtis, Jonathan Battat, Einat Minkov, Jamey Hicks, Seth Teller, and Jonathan Ledlie. 2010. Growing an organic indoor location system. In *Proceedings of the ACM MobiSys*.
[28] Anshul Rai, Krishna Kant Chintalapudi, Venkata N. Padmanabhan, and Rijurekha Sen. 2012. Zee: Zero-effort Crowdsourcing for Indoor Localization. In *Proceedings of the ACM MobiCom*.
[29] Souvik Sen, Bo Radunovic, Romit Roy Choudhury, and Tom Minka. 2012. You are facing the Mona Lisa: spot localization using PHY layer information. In *Proceedings of the ACM MobiSys*.
[30] Guobin Shen, Zhuo Chen, Peichao Zhang, Thomas Moscibroda, and Yongguang Zhang. 2013. Walkie-Markie: indoor pathway mapping made easy. In *Proceedings of the USENIX NSDI*.
[31] Y. Shu, Y. Huang, J. Zhang, P. Cou, P. Cheng, J. Chen, and K. G. Shin. 2016. Gradient-Based Fingerprinting for Indoor Localization and Tracking. *IEEE Transactions on Industrial Electronics* 63, 4 (April 2016), 2424–2433.
[32] Wei Sun, Junliang Liu, Chenshu Wu, Zheng Yang, Xinglin Zhang, and Yunhao Liu. 2013. MoLoc: on distinguishing fingerprint twins. In *Proceedings of the IEEE ICDCS*.
[33] Deepak Vasisht, Swarun Kumar, and Dina Katabi. 2016. Decimeter-level localization with a single WiFi access point. In *Proceedings of the USENIX NSDI*.
[34] He Wang, Souvik Sen, Ahmed Elgohary, Moustafa Farid, Moustafa Youssef, and Romit Roy Choudhury. 2012. No need to war-drive: unsupervised indoor localization. In *Proceedings of the ACM MobiSys*.
[35] Ju Wang, Hongbo Jiang, Jie Xiong, Kyle Jamieson, Xiaojiang Chen, Dingyi Fang, and Binbin Xie. 2016. LiFS: Low Human Effort, Device-Free Localization with Fine-Grained Subcarrier Information. In *Proceedings of ACM MobiCom*.
[36] Jue Wang and Dina Katabi. 2013. Dude, Where's My Card? RFID Positioning That Works with Multipath and Non-Line of Sight. In *Proceedings of the ACM SIGCOMM*.
[37] Chenshu Wu, Zheng Yang, Chaowei Xiao, Chaofan Yang, Yunhao Liu, and Mingyan Liu. 2015. Static Power of Mobile Devices: Self-updating Radio Maps for Wireless Indoor Localization. In *Proceedings of the IEEE INFOCOM*.
[38] Kaishun Wu, J Xiao, Youwen Yi, Min Gao, and L. M Ni. 2012. FILA: Fine-grained indoor localization. In *Proceedings of the IEEE INFOCOM*.
[39] Yaxiong Xie, Zhenjiang Li, and Mo Li. 2015. Precise power delay profiling with commodity wifi. In *Proceedings of the ACM MobiCom*.
[40] Jie Xiong and Kyle Jamieson. 2013. ArrayTrack: A Fine-Grained Indoor Location System.. In *Proceedings of the USENIX NSDI*.
[41] Jie Xiong, Karthikeyan Sundaresan, and Kyle Jamieson. 2015. Tonetrack: Leveraging frequency-agile radios for time-based indoor wireless localization. In *Proceedings of the ACM MobiCom*.
[42] Han Xu, Zheng Yang, Zimu Zhou, Longfei Shangguan, Ke Yi, and Yunhao Liu. 2015. Enhancing Wifi-based Localization with Visual Clues. In *Proceedings of the ACM UbiComp*.
[43] Zheng Yang, Chenshu Wu, and Yunhao Liu. 2012. Locating in Fingerprint Space: Wireless Indoor Localization with Little Human Intervention. In *Proceedings of the ACM MobiCom*.

[44] Zheng Yang, Chenshu Wu, Zimu Zhou, Xinglin Zhang, Xu Wang, and Yunhao Liu. 2015. Mobility Increases Localizability: A Survey on Wireless Indoor Localization Using Inertial Sensors. *Comput. Surveys* 47, 3, Article 54 (April 2015), 34 pages.
[45] Xuehan Ye, Yongcai Wang, Wei Hu, Lei Song, Zhaoquan Gu, and Deying Li. 2016. WarpMap: Accurate and Efficient Indoor Location by Dynamic Warping in Sequence-Type Radio-Map. In *Proceedings of the IEEE SECON*.
[46] Jie Yin, Qiang Yang, and Lionel M Ni. 2008. Learning adaptive temporal radio maps for signal-strength-based location estimation. *Mobile Computing, IEEE Transactions on* 7, 7 (2008), 869–883.
[47] Moustafa Youssef and Ashok Agrawala. 2008. The Horus Location Determination System. *Wireless Networks* 14, 3 (June 2008), 357–374.
[48] Yuanqing Zheng, Guobin Shen, Liqun Li, Chunshui Zhao, Mo Li, and Feng Zhao. 2014. Travi-Navi: Self-deployable Indoor Navigation System. In *Proceedings of the ACM MobiCom*.

Received November 2016; major revision February 2017